

Report

The Egg Surface LDL Receptor Repeat-Containing Proteins EGG-1 and EGG-2 Are Required for Fertilization in *Caenorhabditis elegans*

Pavan Kadandale,¹ Allison Stewart-Michaelis,¹ Scott Gordon,¹ Jacob Rubin,¹ Richard Klancer,¹ Peter Schweinsberg,² Barth D. Grant,² and Andrew Singson^{1,*}

¹Waksman Institute and Department of Genetics

²Department of Molecular Biology and Biochemistry Rutgers University

Piscataway, New Jersey 08854

Summary

The molecular machinery that mediates sperm-egg interactions at fertilization is largely unknown. We identify two partially redundant egg surface LDL receptor repeat-containing proteins (EGG-1 and EGG-2) that are required for *Caenorhabditis elegans* fertility in hermaphrodites, but not males. Wild-type sperm cannot enter the morphologically normal oocytes produced by hermaphrodites that lack *egg-1* and *egg-2* function despite direct gamete contact. Furthermore, we find that levels of meiotic maturation/ovulation and sperm migratory behavior are altered in *egg-1* mutants. These observations suggest an unexpected regulatory link between fertilization and other events necessary for reproductive success. *egg-1* and *egg-2* are the result of a gene duplication in the nematode lineage leading to *C. elegans*. The two closely related species *C. briggsae* and *C. remanei* encode only a single *egg-1/egg-2* homolog that is required for hermaphrodite/female fertility. In addition to being the first identified egg components of the nematode fertilization machinery, the *egg-1* and *egg-2* gene duplication could be vital with regards to maximizing *C. elegans* fecundity and understanding the evolutionary differentiation of molecular function and speciation.

Results and Discussion

Fertilization requires a precise series of cell-cell interactions that include gamete recognition, signaling, binding, and fusion. Despite the fundamental nature of these events, the molecular machinery that mediates sperm-egg interactions at fertilization is largely unknown [1–3]. *C. elegans* is emerging as an important model system for the study of fertilization [4]. Several studies have identified the first sperm components required for fertilization [5–7]. However, to gain a full understanding of fertilization at the molecular level, egg components must also be identified.

We searched the *Caenorhabditis elegans* DNA microarray data set of Reinke et al. [8] for genes that display an oocyte-enriched expression pattern and encode transmembrane molecules with features or motifs known to be involved in ligand-receptor and cell-cell interactions.

One of these genes, *egg-1* (B0244.8), is predicted to encode a type II transmembrane molecule with an extracellular domain that contains an array of eight LDL receptor type A domains (Figures 1A and 1C). In addition to related molecules in many species (often with additional domains), BLAST [9] and SMART [10] analysis identified the existence of a paralogous gene in *C. elegans* (*egg-2*, R01H2.3) that also displays an oocyte-enriched expression pattern. Single orthologs of *egg-1/egg-2* exist in the related nematodes *C. briggsae* (*Cb-egg-1* CBG08534) and *C. remanei* (*Cr-egg-1*, contig 153.1) (Figure 1C) (see Supplemental Experimental Procedures for details of all methods).

To further investigate the expression patterns of the *egg-1* and *egg-2* genes and determine the subcellular localization of their encoded proteins we created transgenic worm strains carrying integrated green fluorescent protein (*gfp*) fusions driven by either the endogenous *egg-1/egg-2* promoters or the *pie-1* promoter [11] (Figure S1a). EGG-1:GFP and EGG-2:GFP driven by their own promoters are restricted to the adult germ line (Figures 1D and 1E) consistent with previous expression data [8, 12]. Further, EGG-1:GFP, EGG-2:GFP (endogenous promoters, C-terminal GFP fusions) and GFP:EGG-1 (*pie-1* promoter, N-terminal GFP fusion) appear to localize to the plasma membrane of developing oocytes (Figures 1D–1I, Figures S1b–S1e). The GFP fusion proteins display a “swiss cheese” appearance (Figure 1F–1I) when viewed at high magnification using 3D-deconvolution microscopy. This is in contrast to the *C. elegans* LDL receptor homolog RME-2 that cycles off the plasma membrane at a high rate with a steady-state enrichment in cortical endosomes [13]. RME-2:GFP displays a punctate and less tightly defined distribution (Figures 1J and 1K). To test for cell surface localization of EGG-1, we developed a live-cell staining assay in which we injected anti-GFP sera into the uterus of hermaphrodites. We observed anti-GFP staining on the surface of oocytes in the proximal gonad arms and uterus of animals expressing the EGG-1:GFP fusion (C-terminal fusion, GFP on surface) (Figures S2A–S2C). Further, this staining colocalized with GFP fluorescence (Figure S2C). No oocyte surface staining was seen with the anti-GFP sera injected into the uterus of hermaphrodites expressing the GFP:EGG-1 (Figure S2D–S2F) (N-terminal fusion, GFP in the cytoplasm). These experiments demonstrate that EGG-1:GFP is on the egg plasma membrane and support the topology of EGG-1 shown in Figure 1C. The surface localization of the EGG-1:GFP fusion proteins are likely to be biologically significant because the GFP:EGG-1 construct can rescue *egg-1* mutant fertility defects (see below). Together, these data support the hypothesis that EGG-1 and EGG-2 are expressed in developing oocytes and reside on the oocyte plasma membrane where they could directly mediate gamete interactions at fertilization.

RNA interference (RNAi) was used to investigate the function of the *egg-1* and *egg-2* genes (Table 1, Figure 2).

*Correspondence: singson@waksman.rutgers.edu

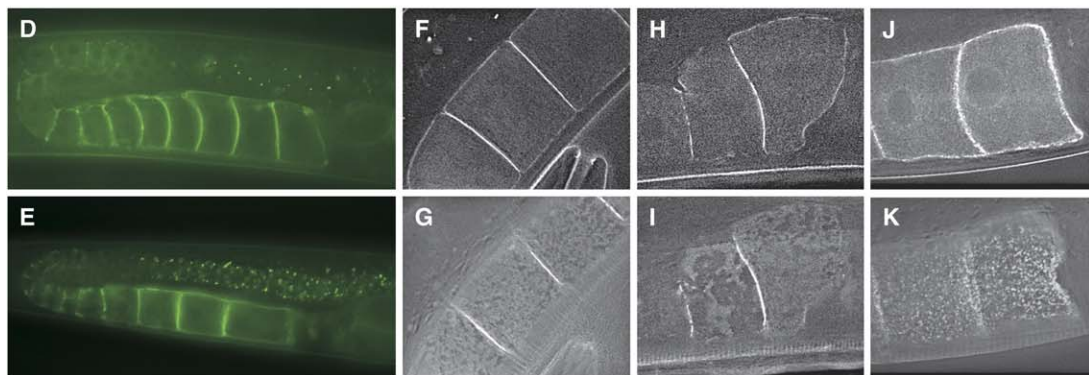
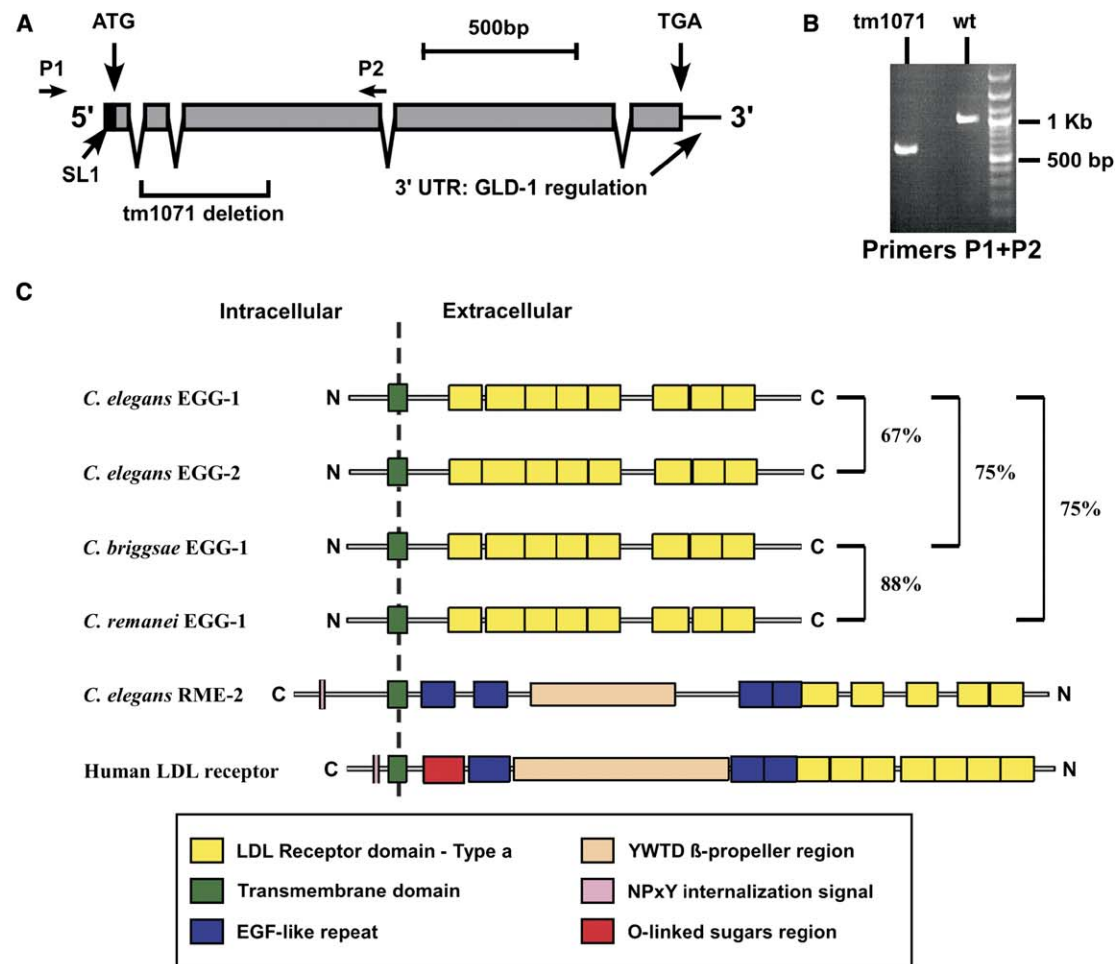


Figure 1. The *egg-1* Gene, Related Proteins, Expression, and Subcellular Localization

(A) *egg-1* genomic structure and the *tm1071* mutation. The position of the *trans*-spliced leader (SL1), the start ATG, and proposed site of GLD-1 translational repressor regulation in the 3' untranslated region (UTR) are indicated. The bracket below indicates the sequences deleted in *tm1071*. The position of primers used for PCR amplifications in (B) are indicated and labeled P1 and P2.

(B) PCR characterization of the *tm1071* deletion mutation shows that the band amplified with primers P1 and P2 is smaller from *tm1071* homozygotes than from wild-type. These PCR products were sequenced to further verify the nature of this mutation.

(C) Visual comparison of the structural organization of the EGG proteins with each other and the worm LDL receptor homolog RME-2 and the human LDL receptor. The percent amino acid identity between EGG proteins is indicated with brackets. Protein motifs are indicated in the boxed key. (D-K) Expression pattern and subcellular localization of EGG-1:GFP (D, F, and G), EGG-2:GFP (E, H, and I), and RME-2:GFP (J and K). The expression of EGG-1:GFP (D) and EGG-2:GFP (E) in the adult gonad and developing oocytes is shown. (F and G) Deconvolved images showing the subcellular localization of EGG-1:GFP ([F], middle focal plane; [G], 10 focal plane stack projection of the cell surface), EGG-2:GFP ([H], middle; [I], surface), and RME-2:GFP ([J], middle; [K], surface/cortex). The tight localization of EGG-1/EGG-2:GFP to the plasma membrane is very different from that of RME-2 which accumulates in cortical endosomes at a steady-state [13].

Table 1. Fertility Defects and Summary of Phenotypes

RNAi Experiments			
RNAi Treatment	Temperature	Unfertilized Oocytes	
Mock RNAi	25°C	No	
<i>egg-1</i> (B0244.8) RNAi	25°C	Yes	
<i>egg-2</i> (R01H2.3) RNAi	25°C	Yes	
<i>C. briggsae</i> , mock RNAi	25°C	No	
<i>C. briggsae</i> , <i>Cb-egg-1</i> RNAi	25°C	Yes	
<i>C. remanei</i> , mock RNAi	25°C	No	
<i>C. remanei</i> , <i>Cr-egg-1</i> RNAi	25°C	Yes	
Mutant Hermaphrodite Fertility			
Genotype	Temperature	Brood Percentage Wild-Type ± SD	Ovulations Percentage Wild-Type ± SD
<i>egg-1(tm1071)</i>	25°C	6 ± 4	10 ± 4
<i>egg-1(tm1071)</i>	20°C	54 ± 13	44 ± 10
<i>egg-1(tm1071)</i>	16°C	91 ± 18	80 ± 16
<i>egg-1(tm1071); gfp:egg-1 Rescue</i>	25°C	25 ± 23	25 ± 19
<i>fem-1(e1965)</i> no sperm control	25°C	0	6 ± 3
Fertility Phenotypes			
Events or phenotype	Wild-type	<i>egg-1 (tm1071)</i>	
Male fertility*	+	+	
Gonad morphology (male and hermaphrodite)	+	+	
Gamete morphology (sperm and oocytes)	+	+	
Germ line/oocyte cell cycle progression	+	+	
Fat metabolism (Nile Red staining assay)	+	+	
Yolk uptake/oocyte growth volume increase	+	+	
Disappearance of nucleolus	+	+	
Distal nuclear migration	+	+	
Nuclear envelope breakdown (NEBD)	+	+	
Cortical rearrangement	+	+	
Ovulation	+	+	
Oocyte contact with sperm in spermatheca	+	+	
Sperm activation (spermiogenesis)	+	+	
Sperm in spermatheca < one day after L4	+	+	
Sperm in spermatheca > one day after L4	+	-	
Entry of sperm pronuclei	+	-	
Egg shell formation	+	-	
Embryogenesis	+	-	
Endomitosis in gonad arm	-	-	
Endomitosis in uterus	-	+	

Broods were determined for animals of the indicated genotype by counting the number of progeny and ovulations (fertilized eggs and unfertilized oocytes produced). Broods are indicated as percentage of wild-type controls raised under identical culture or treatment conditions. All experiments were conducted on *C. elegans* except where indicated. *Male *egg-1; him-5* fertility was determined by crossing into *dpy-5* hermaphrodites and scoring the number of Non-Dpy (outcross) progeny produced. *egg-1; him-5* mutant male fertility was similar to *him-5* (see Figure 4). SD = standard deviation

Hermaphrodites became completely sterile and produced only unfertilized oocytes when double-stranded (ds) RNA corresponding to *egg-1* was injected at 25°C (Figure 2B). No fertility was recovered when these animals were crossed to wild-type males. Furthermore, these sterile worms did not display any detectable gametogenesis or somatic defects (Table 1, see below), and no fertility defects were detected in mock-injected controls (Table 1, Figure 2A). These results were consistent with RNAi findings from a large-scale RNAi soaking screen [14] and a study to identify GLD-1 translational repressor targets in the germ line [12]. We also detected reduced fertility and the production of unfertilized oocytes when dsRNA corresponding to *egg-2* was delivered by feeding at 25°C (Table 1, Figure 2C). The effectiveness of various RNAi treatments was monitored with the GFP reporters for *egg-1* and *egg-2* (Figures 2F–2I). *egg-1* RNAi not only knocked down EGG-1:GFP but also knocked down EGG-2:GFP. *egg-2* RNAi effectively knocked down EGG-2:GFP. Therefore the strong fertility defects seen in *egg-1* RNAi treated animals is likely due to cross-RNAi effects. Injection RNAi at 25°C of the *C. briggsae egg-1 (Cb-egg-1)* or the *C. remanei egg-1 (Cr-egg-1)* homologs also resulted in the production of unfertilized oocytes (Figures 2D and 2E) in the respective species. This result suggests that these genes have a conserved fertility function in nematodes.

To test the validity of our RNAi induced phenotypes for *egg-1*, we obtained a deletion allele from the National Bioresource Project for the Nematode, Japan. The *egg-1 (tm1071)* allele carries a 416 base pair deletion (Figures 1A and 1B) that removes the genomic region from intron 1 to approximately half-way through exon 3. The resulting mutant gene is predicted to encode only the first 24 amino acids of the protein. The knockout worms are not as sterile as worms treated with *egg-1* RNAi. This mutation is recessive and homozygous hermaphrodites display temperature sensitive fertility defects (Table 1). At 25°C, mutant hermaphrodite fertility is only 6% of wild-type fertility and unfertilized oocytes accumulate in the uterus of these animals (Figure 3A). Based on our RNAi phenotypes, residual fertility is due to *egg-2* function in *egg-1(tm1071)* mutants. Fertility levels are partially rescued by the *gfp:egg-1* construct (Table 1). Incomplete rescue could be due to germ line transgene silencing [15, 16] or reduced activity of the fusion protein due to the presence of GFP sequences.

Mutant hermaphrodites produce morphologically wild-type sperm and oocytes (Table 1, Figures 3A–3D, 4C and 4D). In young *egg-1* mutants, oocyte meiotic maturation/ovulation occurs and brings sperm and oocytes in contact in the spermatheca (the normal site of fertilization, Figures 3B–3D). However, no fertilization occurs and no sperm DNA is detected in DAPI-stained oocytes dissected from the uterus of *egg-1* mutants (Figures 3F and 3G). These unfertilized oocytes become endomitotic as they age (Figure 3H). This data suggest that fertility defects are not due to defective gamete production. Occasionally slightly abnormal/damaged or fragmented oocytes can be seen in some preparations of RNAi-treated or mutant worms. However, these abnormalities are not consistently associated with *egg* gene loss of function and are likely due to experimental manipulations (e.g., injection or mounting) or low ovulation

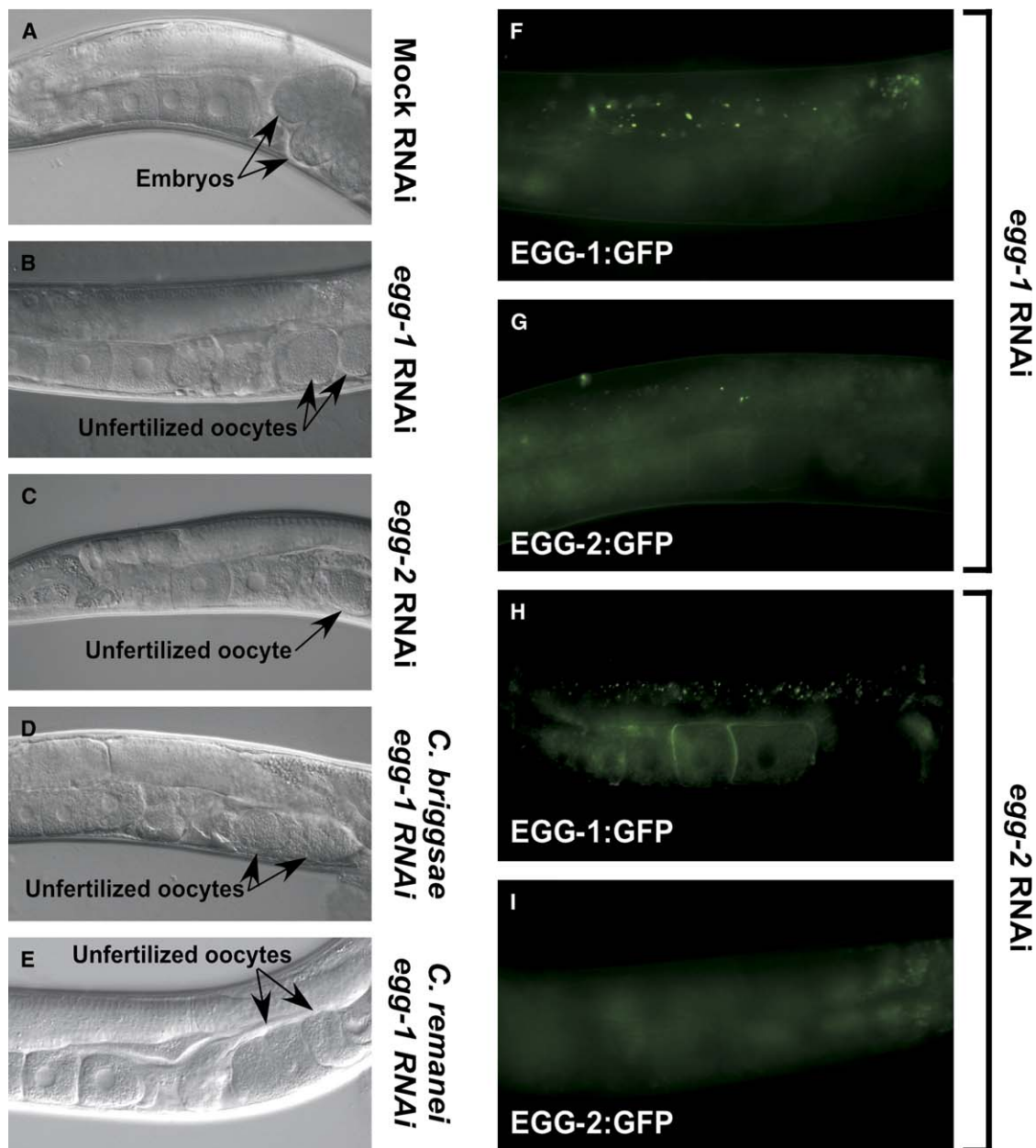


Figure 2. RNAi Knockdown of *Ce-egg-1*, *Ce-egg-2*, *Cb-egg-1*, and *Cr-egg-1*

(A–E) Phenotypic effects of RNAi. (A) Mock RNAi worms are wild-type and accumulate developing embryos in the uterus. RNAi against *Ce-egg-1* (B), *Ce-egg-2* (C), *Cb-egg-1* (D), or *Cr-egg-1* (E) results in the accumulation of unfertilized oocytes in the uterus of treated animals. (F–I) The effectiveness and cross-RNAi effects can be monitored by GFP fluorescence. *Ce-egg-1* RNAi depletes both EGG-1:GFP (F) and EGG-2:GFP (G). *Ce-egg-2* RNAi effects on EGG-1:GFP (H) and EGG-2:GFP (I).

rates (see below) since we can observe similar defects in preparations of wild-type worms. Although we cannot rule out the possibility of a subtle defect in oogenesis, detailed examination of both wild-type and *egg* gene loss of function animals reveal no obvious and consistently associated phenotypic defects (Table 1. see fertility phenotypes) [17].

Homozygous *egg-1* males have no detectable somatic or fertility defects (Figures 4A–4D). They sire broods that are comparable in number to wild-type males (Figure 4A) indicating that mating behavior, sperm transfer, sperm migratory behavior, and sperm competition are normal

for sperm produced by these mutant males [4, 6, 18]. In vitro sperm activation and amoeboid sperm morphology are also indistinguishable from wild-type (Figures 4B–4D) and no EGG-1:GFP or EGG-2:GFP expression is seen (data not shown) in males consistent with microarray data [8]. Essentially identical results are obtained when we also knockdown *egg-2* function with RNAi in an *egg-1(tm1071)* mutant background (Figure S3).

egg-1 hermaphrodites ovulate at levels that are considerably lower than wild-type controls (Table 1), and oocytes can be observed backing up in the gonad arm of older hermaphrodites (Figure 3E). High levels of

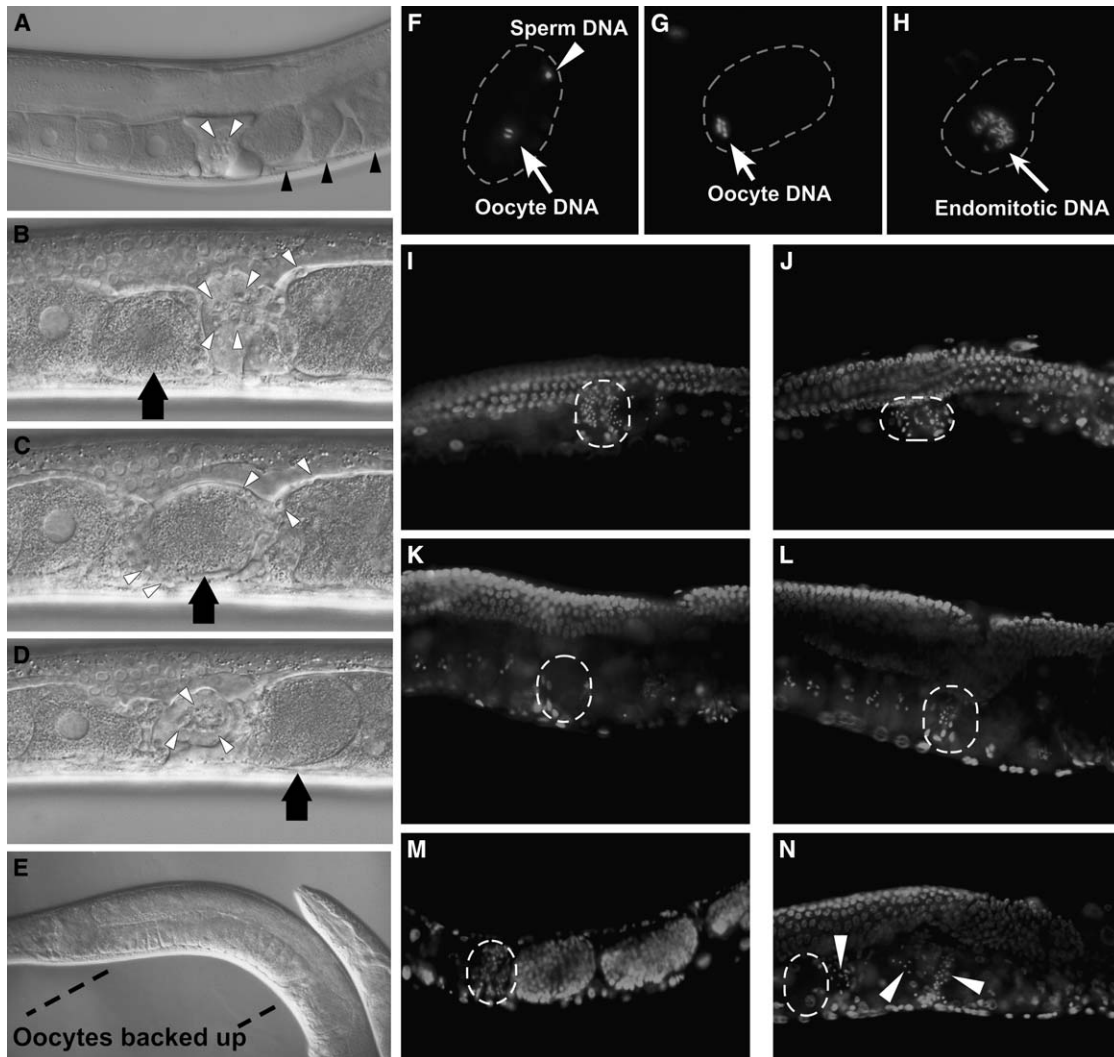


Figure 3. Phenotypes of the *egg-1(tm1071)* Mutant

In all panels, white arrowheads indicate examples or the position of sperm or sperm DNA. White arrows indicate oocyte DNA. Black arrows indicate the position of oocytes. Black arrowheads indicate the position of unfertilized oocytes. Dashed lines indicate the outline of oocytes or the position of the spermatheca. For panels showing intact hermaphrodites, the oviduct is on the left and the uterus is on the right.

(A) Unfertilized oocytes accumulate in the uterus of a young *egg-1* mutant despite passing through a sperm-containing spermatheca.

(B–D) Three sequential Nomarski DIC micrographs showing ovulation and sperm-oocyte contact in the spermatheca of a young *egg-1* hermaphrodite. The large black arrow indicates the position of a single oocyte as it moves from the oviduct (after nuclear envelope breakdown and cortical rearrangement) (B), to the spermatheca (C), and the uterus (D).

(E) Oocytes back up in the gonad arm of older *egg-1* hermaphrodites indicating lowered levels of oocyte meiotic maturation and ovulation.

(F) Sperm and oocyte DNA can be detected in DAPI stained oocytes dissected from the uterus of wild-type hermaphrodites.

(G) Oocyte DNA but no sperm DNA can be observed in unfertilized oocytes dissected from the uterus of an *egg-1* hermaphrodite.

(H) These oocytes become endomitotic as they age.

(I–N) Sperm detected as small bright DAPI stained spots can be found in the spermatheca of young *egg-1* (I) and wild-type (J) hermaphrodites. However, sperm are lost from the spermatheca of older (> one day) *egg-1* mutant hermaphrodites (K) when compared to age matched wild-type (L) controls. In *let-23* single mutants (M), sperm can be detected in the spermatheca while sperm are only detected in the uterus of age-matched *let-23, egg-1* double mutants (N).

meiotic maturation and ovulation are known to require a sperm-sensing mechanism. Mutants that are defective in this mechanism (that is likely dependent on sperm vesicle budding) [19, 20] or lack sperm [17] (Table 1, see *fem-1*) exhibit low meiotic maturation/ovulation level phenotypes similar to those seen in *egg-1* mutants. In our *egg-1* mutants, at least part of the reduced ovulation levels is due to a surprising and rapid loss of sperm (and thus a loss of signal) from the *egg-1* mutant

reproductive tract (Figures 3I–3L). In wild-type hermaphrodites, many sperm are displaced from the spermatheca to the uterus by passing eggs. These sperm then ignore the contents of the uterus and crawl back into the closest spermatheca. In anesthetized *egg-1* hermaphrodites, we observed that sperm were not efficiently crawling back into the spermatheca after being pushed into the uterus by passing oocytes. Rather, sperm were expelled from the uterus when oocytes

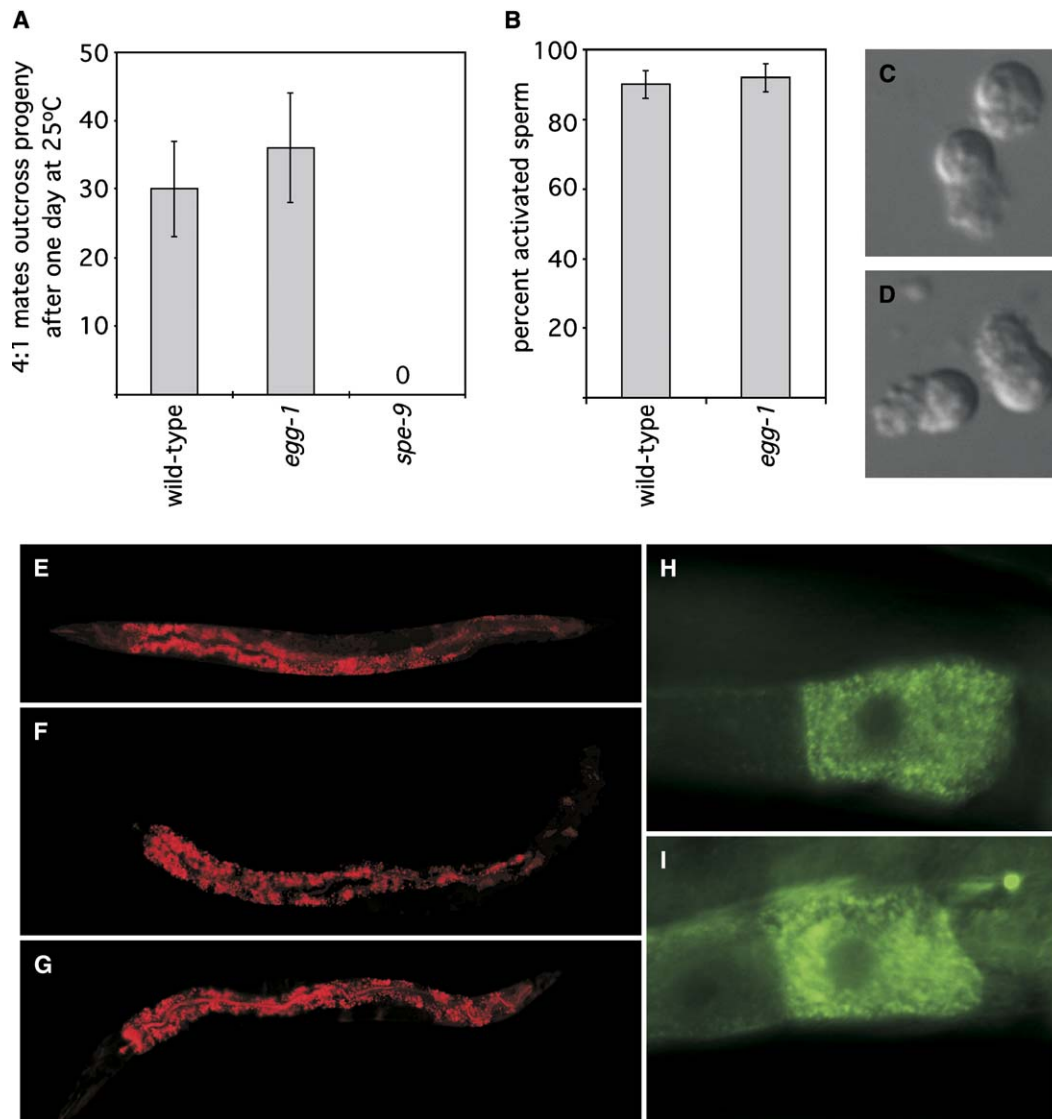


Figure 4. *egg-1(tm1071)* Male Fertility, Sperm Activation, Morphology, Fat Metabolism, and Oocyte Endocytosis

(A) *egg-1* mutant males sire broods that are comparable in number to wild-type. This result is in sharp contrast to *spe-9* “sperm sterile” mutants that sire no outcross progeny.

(B) In vitro-activated *egg-1* mutant sperm activate at wild-type levels. Sperm dissected from males of the indicated genotype were activated with Pronase [6], and the percent of activated sperm was determined by counting the total number of sperm with pseudopods and the total number of spermatids.

(C and D) The amoeboid sperm morphology of sperm produced by *egg-1* mutants (C) is indistinguishable from sperm produced by wild-type (D) animals. Error bars in (A) and (B) represent the standard deviation. Fat metabolism (E–G) and oocyte endocytosis (H and I) in *egg* mutants is indistinguishable from wild-type. Vital dye Nile Red staining reflects overall fat content in *C. elegans* [25]. We find that Nile Red accumulation is identical in wild-type (E), *egg-1(tm1071)* mutants (F), and *egg-2* RNAi-treated (G) animals. The YP170:GFP fusion only enters oocytes by endocytosis [13].

(H and I) Both wild-type (H) and *egg-1(tm1071)* (I) animals produce oocytes that accumulate YP170:GFP.

were laid. To gain a better understanding of this sperm loss, we examined sperm localization in a *let-23(sy1)* mutant background. *let-23* mutants lack a vulva, precluding exit of any sperm, embryos, or unfertilized oocytes from the reproductive tract. Although sperm are localized to the spermatheca in *let-23* mutants (Figure 3M), in *let-23; egg-1* double mutants sperm are distributed throughout the uterus (Figure 3N). This demonstrates that *egg-1* mutant worms are not efficiently maintaining a concentrated sperm population in the spermatheca. These data indicate the existence of

previously-unappreciated layers of feedback regulation that help coordinate sperm migratory behavior and the proper levels of meiotic maturation/ovulation with successful fertilization. Work with other fertility mutants has suggested that there are indeed differential effects on the coordination of fertilization with meiotic maturation/ovulation rates in *C. elegans* [21].

LDL receptor-related molecules are known to bind diverse ligands (e.g., lipoproteins, viruses, and signaling factors) and mediate diverse cellular activities (e.g., endocytosis, Ca^{2+} influx, and synaptic plasticity) [22].

Defects in LDL receptor repeat-containing molecules are associated with various human diseases [22, 23] and defects in worm development [13, 24]. To our knowledge, this is the first time that LDL receptor-related molecules have been shown to play a role in gamete interactions. Because a number of LDL receptor-related molecules in *C. elegans* have been implicated in fat metabolism [25] and yolk uptake [13], we assayed for possible defects in these processes. Knockout or RNAi-treated animals did not display any fat metabolism defects using the assay developed by Ashrafi et al. [25] that reflects overall fat metabolism (Figures 4E–4G). Oocyte endocytosis was also normal in *egg-1* knockout animals as assayed by (yolk protein) YP170:GFP uptake [13] (Figures 4H and 4I). Although EGG-1 and EGG-2 ligands are likely to be independent of fat metabolism and yolk uptake, we can't rule out defects in alternate transport pathways. However, these defects would have to be subtle because as noted earlier, *egg-1/egg-2* mutant oocyte growth/morphology are indistinguishable from wild-type and the localization of our GFP reporters (unlike RME-2) are not consistent with high rates of internalization.

The molecular nature of the predicted EGG-1 and EGG-2 proteins suggests a model in which their arrays of LDL receptor repeats are displayed on the oocyte surface where they can bind to a sperm ligand(s). Such interactions would then be required for successful fertilization. The Human LDL receptor and its *C. elegans* homolog [13, 23] have sequences required for targeting to clathrin-coated pits (NPxY) and endosome ligand release [23] (EGF repeat- β -Propeller region) (Figure 1C). The fact that the predicted EGG-1 and EGG-2 proteins lack these sequences suggests why these proteins remain on the plasma membrane at a steady-state and that ligand binding at the oocyte surface would not include endocytosis of ligand-receptor complexes or ligand release in endosomes. Recent studies have provided evidence that *C. elegans* sperm fuse with the oocyte plasma membrane rather than being engulfed (A. Richmond and D. Shakes, personal communication).

C. elegans expresses two structurally related proteins (Ce-EGG-1 and Ce-EGG-2) that function in a partially redundant fashion. *C. briggsae* (Cb-EGG-1) and *C. remanei* (Cr-EGG-1) have only a single predicted protein of this type (Figure 1C). An extra copy/variant of an egg surface sperm receptor could enhance *C. elegans* fertility or provide more robust gamete interactions across a larger range of environmental conditions (e.g., different temperatures). Phylogenetic analysis of the *egg-1* and *egg-2* genes suggests that the *egg-1* ancestor gene duplicated in the nematode lineage leading to *C. elegans* after it split from its last common ancestor with *C. briggsae* and *C. remanei* (Figure S4). In addition to understanding the implications and mechanisms of gene duplication [26, 27], there is intense interest in understanding the evolution of gamete interaction protein function [28]. Other LDL receptor repeat-containing molecules are known to function specifically in other oocyte functions such as yolk uptake [13]. An intriguing possibility is that *egg-1/egg-2* could have arisen from one of these functions in the oocyte. Continued analysis of these genes will lead to a better understanding of the differentiation of molecular functions and how modification

of gamete interactions at the molecular level could contribute to speciation.

Supplemental Data

Supplemental Data includes four figures and Supplemental Experimental Procedures and can be found with this article online at <http://www.current-biology.com/cgi/content/full/15/24/2222/DC1/>.

Acknowledgments

We thank Monica Driscoll, Chi-hua Chiu, David Greenstein, and members of the Singson Lab for discussions and suggestions. We thank Chris Rongo for reagents and assistance with live cell-staining protocols. P.K. was supported by a Charles and Johanna Busch predoctoral fellowship. Work in the Singson lab is supported by grants from the National Institutes of Health (NIH) (R01 GM63089), Johnson and Johnson Discovery Award, and funds from the Rutgers College Undergraduate Honors and Henry Rutgers Undergraduate Honors program. Work in the Grant lab is supported by a grant from the NIH (R01 GM067237). We acknowledge the Mitani Lab and National Bioresource Project for the nematode Japan for kindly providing the *egg-1(tm1071)* mutation and the Kohara Lab for providing cDNA clones. We also thank Asako Sugimoto for attempting to find alleles of *egg-1* in her deletion library. The *Caenorhabditis* Genetics Center provided several strains and is funded by the NIH National Center for Research Resources (NCRR).

Received: August 3, 2005

Revised: October 5, 2005

Accepted: October 19, 2005

Published: December 19, 2005

References

1. Geldziler, B., Kadandale, P., and Singson, A. (2004). Molecular genetic approaches to studying fertilization in model systems. *Reproduction* 127, 409–416.
2. Primakoff, P., and Myles, D.G. (2002). Penetration, adhesion, and fusion in mammalian sperm-egg interaction. *Science* 296, 2183–2185.
3. Schultz, R., and Williams, C. (2005). Developmental biology: sperm-egg fusion unscrambled. *Nature* 434, 152–153.
4. Singson, A. (2001). Every sperm is sacred: fertilization in *Caenorhabditis elegans*. *Dev. Biol.* 230, 101–109.
5. Chatterjee, I., Richmond, A., Putiri, E., Shakes, D.C., and Singson, A. (2005). The *Caenorhabditis elegans spe-38* gene encodes a novel four-pass integral membrane protein required for sperm function at fertilization. *Development* 132, 2795–2808.
6. Singson, A., Mercer, K.B., and L'Hernault, S.W. (1998). The *C. elegans spe-9* gene encodes a sperm transmembrane protein that contains EGF-like repeats and is required for fertilization. *Cell* 93, 71–79.
7. Xu, X.Z., and Sternberg, P.W. (2003). A *C. elegans* sperm TRP protein required for sperm-egg interactions during fertilization. *Cell* 114, 285–297.
8. Reinke, V., Gil, I.S., Ward, S., and Kazmer, K. (2004). Genome-wide germline-enriched and sex-biased expression profiles in *Caenorhabditis elegans*. *Development* 131, 311–323.
9. Altschul, S.F., Gish, W., Miller, W., Myers, E.W., and Lipman, D.J. (1990). Basic local alignment search tool. *J. Mol. Biol.* 215, 403–410.
10. Schultz, J., Copley, R.R., Doerks, T., Ponting, C.P., and Bork, P. (2000). SMART: a web-based tool for the study of genetically mobile domains. *Nucleic Acids Res.* 28, 231–234.
11. Tenenhaus, C., Schubert, C., and Seydoux, G. (1998). Genetic requirements for PIE-1 localization and inhibition of gene expression in the embryonic germ lineage of *Caenorhabditis elegans*. *Dev. Biol.* 200, 212–224.
12. Lee, M.H., and Schedl, T. (2001). Identification of in vivo mRNA targets of GLD-1, a maxi-KH motif containing protein required for *C. elegans* germ cell development. *Genes Dev.* 15, 2408–2420.

13. Grant, B., and Hirsh, D. (1999). Receptor-mediated endocytosis in the *Caenorhabditis elegans* oocyte. *Mol. Biol. Cell* 10, 4311–4326.
14. Maeda, I., Kohara, Y., Yamamoto, M., and Sugimoto, A. (2001). Large-scale analysis of gene function in *Caenorhabditis elegans* by high-throughput RNAi. *Curr. Biol.* 11, 171–176.
15. Putiri, E., Zannoni, S., Kadandale, P., and Singson, A. (2004). Functional domains and temperature-sensitive mutations in SPE-9, an EGF repeat-containing protein required for fertility in *Caenorhabditis elegans*. *Dev. Biol.* 272, 448–459.
16. Seydoux, G., and Schedl, T. (2001). The germline in *C. elegans*: origins, proliferation, and silencing. *Int. Rev. Cytol.* 203, 139–185.
17. McCarter, J., Bartlett, B., Dang, T., and Schedl, T. (1999). On the control of oocyte meiotic maturation and ovulation in *C. elegans*. *Dev. Biol.* 205, 111–128.
18. Singson, A., Hill, K.L., and L'Hernault, S.W. (1999). Sperm competition in the absence of fertilization in *Caenorhabditis elegans*. *Genetics* 152, 201–208.
19. Kosinski, M., McDonald, K., Schwartz, J., Yamamoto, I., and Greenstein, D. (2005). *C. elegans* sperm bud vesicles to deliver a meiotic maturation signal to distant oocytes. *Development* 132, 3357–3369.
20. Miller, M.A., Ruest, P.J., Kosinski, M., Hanks, S.K., and Greenstein, D. (2003). An Eph receptor sperm-sensing control mechanism for oocyte meiotic maturation in *Caenorhabditis elegans*. *Genes Dev.* 17, 187–200.
21. Kadandale, P., and Singson, A. (2004). Oocyte production and sperm utilization patterns in semi-fertile strains of *Caenorhabditis elegans*. *BMC Dev. Biol.* 4, 3.
22. Nykjaer, A., and Willnow, T.E. (2002). The low-density lipoprotein receptor gene family: a cellular Swiss army knife? *Trends Cell Biol.* 12, 273–280.
23. Innerarity, T.L. (2002). Structural biology. LDL receptor's beta-propeller displaces LDL. *Science* 298, 2337–2339.
24. Kamikura, D.M., and Cooper, J.A. (2003). Lipoprotein receptors and a disabled family cytoplasmic adaptor protein regulate EGL-17/FGF export in *C. elegans*. *Genes Dev.* 17, 2798–2811.
25. Ashrafi, K., Chang, F.Y., Watts, J.L., Fraser, A.G., Kamath, R.S., Ahringer, J., and Ruvkun, G. (2003). Genome-wide RNAi analysis of *Caenorhabditis elegans* fat regulatory genes. *Nature* 421, 268–272.
26. He, X., and Zhang, J. (2005). Gene complexity and gene duplicability. *Curr. Biol.* 15, 1016–1021.
27. Long, M., Thornton, K., Zhang, L., Gaut, B.S., and Vision, T.J. (2001). Gene duplication and evolution. *Science* 293, 1551.
28. Vacquier, V.D. (1998). Evolution of gamete recognition proteins. *Science* 281, 1995–1998.